Transport Of Surface-Modified Nanoparticles Through Cell Monolayers

Annette M. Koch,[b] Fred Reynolds,[a] Hans P. Merkle,[b] Ralph Weissleder,[a] and Lee Josephson*[a]

We synthesized three peptides, a D-polyarginyl peptide (r8(FITC)), a Tat peptide (Tat(FITC)), and a control peptide (Cp(FITC)) and attached each to amino-CLIO, a nanoparticle 30 nm in diameter. We then examined the effective permeability, P_{eff}, of all six materials through CaCo-2 monolayers. The transport of peptide–nanoparticles was characterized by a lag phase (0–8 h) and a steady-state phase (9–27 h). The steady-state P_{eff} values for peptides were in the order r8(FITC) > Tat(FITC) = Cp(FITC). When r8(FITC) and Tat(FITC) peptides were attached to the nanoparticle, they conferred their propensity to traverse cell monolayers onto the nanoparticle, whereas Cp(FITC) did not. Thus, when the r8(FITC) peptide was attached to the amino-CLIO nanoparticle, the resulting peptide–nanoparticle had a P_{eff} similar to that of this poly-D-arginyl peptide alone. The P_{eff} of r8(FITC)–CLIO ($M_W \sim 1000$ kDa) was similar to that of mannitol ($M_W = 182$ Da), a poorly transported reference substance, with a far lower molecular weight. These results are the first to indicate that the modification of nanoparticles by attachment of membrane-translocating sequence-based peptides can alter nanoparticle transport through monolayers. This suggests that the surface modification of nanoparticles might be a general strategy for enhancing the permeability of drugs and that high-permeability nanoparticle-based therapeutics can be useful in selected pharmaceutical applications.

Introduction

Barriers to the movement of molecules, presented either by the plasma membrane or in the form of epithelial or endothelial layers of cells, preclude the use of many bioactive substances as pharmaceuticals. Various types of nano- or microparticles have been proposed as vehicles for transporting drugs across the blood brain barrier,[1,2] across the nasal mucosal epithelium,[3,4] across the intestinal epithelial barriers,[5,6,7] and for topical delivery.[8–10] The covalent attachment of peptidic membrane-translocating sequences (MTSs), peptides with the ability to pass through membranes, to nanoparticles could yield a wide variety of new pharmaceuticals. The MTS of the HIV Tat protein (Tat peptide) has been used to obtain membrane-permeable forms of cyclosporine[11] and radiopharmaceuticals with increased potency,[12] for DNA-based gene therapies[13,14] and for a variety of other applications.[15] A second use of the Tat peptide is in imaging cells used for cell-based therapies. Here cells are labeled ex vivo with Tat peptide–nanoparticle conjugates, followed by their administration and tracking in living systems.[16–18] Cell-based therapies include neuroprogenitor cell implantation to overcome neurological disease, stem-cells injection for bone-marrow reconstitution, and the injection of cells for restoring blood cells (platelets, leukocytes, red blood cells).

A magnetic nanoparticle, Tat-CLIO, has been used to load cells so they can be tracked in vivo by MRI. Tat-CLIO consists of a superparamagnetic iron oxide core and a coating of cross-linked dextran (CLIO, cross-linked iron oxide) to which Tat-peptides are attached at high valency (about 20 peptides per 2064 iron atoms per nanoparticle, see ref. [19]). The nanoparticle features attached fluorochromes to follow its disposition by techniques like FACS or fluorescence microscopy, and a magnetic core that can be tracked by MRI. Tat-CLIO is internalized by a variety of cells, and has been used to track hematopoietic stem cells and antigen-specific T lymphocytes.[16,17]

Understanding the feasibility of using Tat-based materials for pharmaceutical applications is complicated by the diversity of chemically different Tat-based materials and the variety of the systems in which they can be studied. Tat-like materials include: i) Tat-like peptides (including polyarginyl peptides) labeled with metal chelates or fluorochromes ($M_W <$ 3 kDa),[11,12,20,21] ii) Tat-derivatized enzymes (10–500 kDa),[22–24] and iii) Tat-based nanoparticles or liposomes (ca. 1000 kDa).[16,18,25] We therefore chose to study the transport through CaCo-2 monolayers of two distinctly different types of Tat-based materials, Tat-like peptides and peptide–nanoparticle conjugates made by the attachment of Tat-like peptides to the amino-CLIO nanoparticle. Three peptides were employed: i) Tat(FITC) bearing the membrane-translocating sequence of the HIV Tat protein, ii) a D-polyarginyl peptide (r8(FITC)), which has been reported to have superior membrane-translocating properties compared to Tat peptides,[26–28] and iii) a negatively charged control peptide (Cp(FITC)). The nanoparticle used for

[a] *Dr. F. Reynolds, Prof. Dr. R. Weissleder, Prof. Dr. L. Josephson*
Center for Molecular Imaging Research
Massachusetts General Hospital/Harvard Medical School
Building 149, 13th Street, Charlestown, MA 02129 (USA)
Fax: (+1) 617-726-5708
E-mail: ljosephson@partners.org

[b] *Dr. A. M. Koch, Prof. Dr. H. P. Merkle*
Department of Chemistry and Applied BioSciences
Drug Formulation and Delivery
Swiss Federal Institute of Technology Zürich (ETH Zürich)
Winterthurerstraße 190, 8057 Zürich (Switzerland)

 DOI: 10.1002/cbic.200400174

peptide attachment was amino-CLIO, which has been widely used for the attachment of biomolecules.[29,30] Concentrations of peptides or peptide–nanoparticles were determined by using an immunoassay that recognized FITC; this avoided the need to synthesize radiolabeled forms of the six compounds (three peptides, three peptide–nanoparticles) used in this study.[31] In addition, we wanted to follow relatively slow transport processes for times up to 44 h, at which time the probability of some degree of dechelation becomes substantial. The FITC immunoassay employed stable FITC-labeled peptides and peptide–nanoparticles and was performed in microtiter-plate format, thus permitting rapid assaying of large batches of samples.

There are now several reports that the attachment of MTS peptides to enzymes or nanoparticles leads to the transport of these materials through endothelial barriers after intravenous injection.[22,24,32] Though these experiments indicate that MTS attachment affects cell permeation in vivo, compared to the control material without MTS attached, it is difficult to quantitate the amount of transport or compare it to the transport of other substances. Therefore we describe here the transport of Tat-like peptides and the peptide–nanoparticle conjugates made with those peptides through CaCo-2 monolayers. The CaCo-2 model is a well-established epithelial model and is often used to measure the permeability of substances, compare the permeability of unknowns with well-established controls, and estimate bioavailability.[33,34]

We show that the transport of peptide–nanoparticle conjugates through monolayers is strongly dependent on the surface of the nanoparticle, determined by the nature of the attached peptide. These results suggest that libraries of surface-functionalized nanoparticles could be synthesized and screened as we have described[35] in order to obtain still more permeable nanoparticles. Cell-permeable nanoparticles might be considered for the delivery of agents that are therapeutically effective even when only slowly transported through cell layers.

Results

A schematic representation of the synthesis and structure of the peptide–nanoparticle conjugates we employed is shown for the Tat(FITC)–CLIO nanoparticle in Scheme 1, which is derived from ref. [36] All peptides had a common C-terminal sequence of amino acids (-GYK(FITC)C-NH_2) and were attached to the amino-CLIO nanoparticle through C-terminal cysteine and a thioether linkage. The differences in peptide transport therefore reflected the number and nature of the N-terminal amino acids. Peptide–nanoparticles differed from the parent peptides

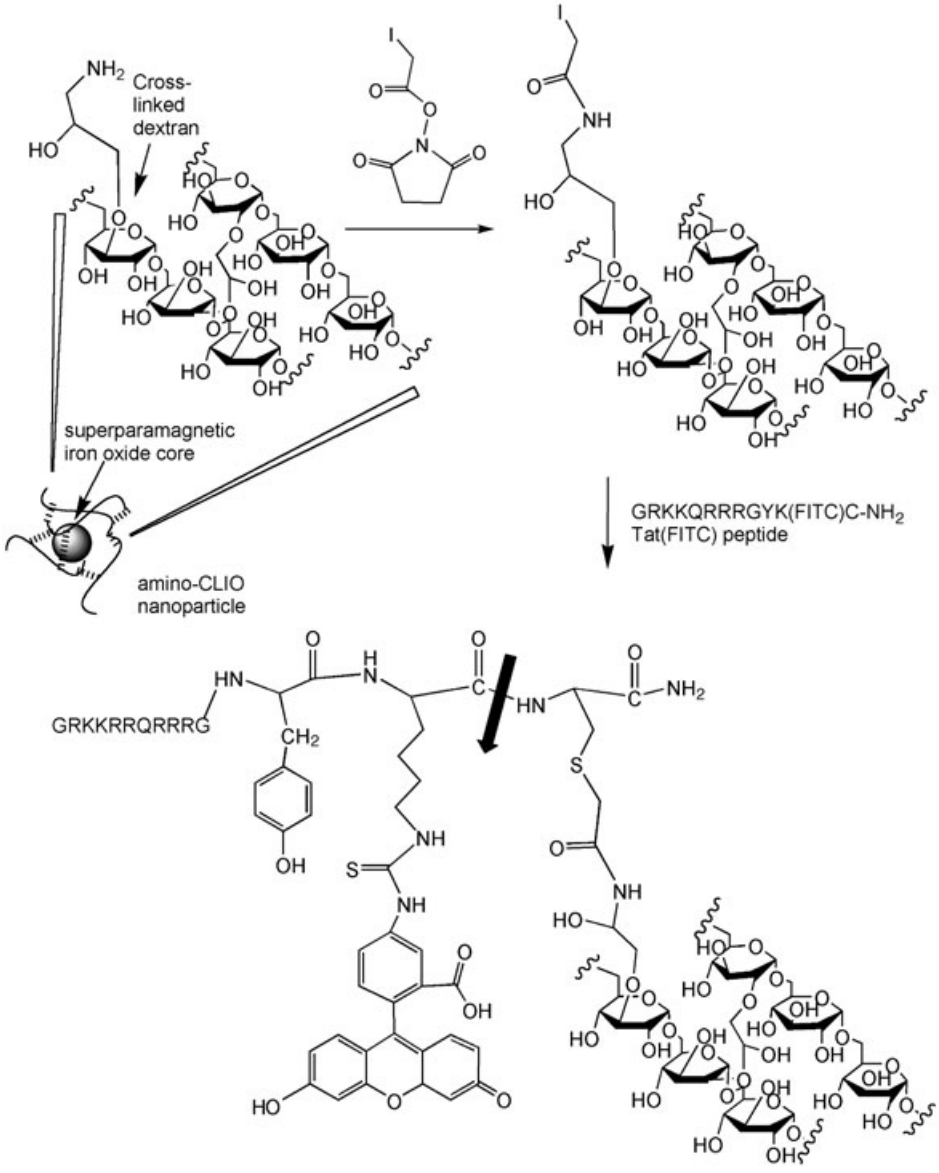

Scheme 1. *Synthesis and features of peptide–nanoparticle conjugates. Amino groups on the cross-linked dextran coating of the nanoparticle were activated with succinimidyl iodoacetate (SIA). Addition of one of three peptides (Cp(FITC): GDSDSGYK(FITC)C-NH_2, Tat(FITC): GRKKRRQRRRGYK(FITC)C-NH_2, or r8(FITC): GrrrrGrrrrGYK(FITC)C-NH_2) resulted in a thioether linkage between the C-terminal cysteine and the nanoparticle. FITC was attached to the epsilon amino group of the penultimate C-terminal lysine residue. Only a protease capable of cleaving the peptide bond (bold arrow) between a FITC-modified lysine and a modified cysteine can separate fluorescein from the nanoparticle. Cleavage of the peptide bonds of the GRKKRRQRRRG sequence does not result in the release of the fluorescein from the nanoparticle.*

both in terms of size (~1000 kDa versus less than 3 kDa) and by the valency of peptide attachment. Peptides are monovalent while the Tat(FITC)–CLIO, r8(FITC)–CLIO, and Cp(FITC)–CLIO nanoparticles had average peptide-to-nanoparticle ratios of 21 ± 6, 20 ± 5, and 18 ± 7, respectively. The side chain of the penultimate lysine was modified by treatment with FITC and the C-terminal cysteine was modified by adding nanoparticles. The stability of the linkage between FITC and the nanoparticle was shown after internalization by HeLa cells. We have shown that HeLa cells retain FITC attached to nanoparticle through the peptide, see Scheme 1, and a Cy3.5 dye attached directly to the cross-linked dextran in a similar manner.[36] In addition, in vitro, fluorescein cannot be separated from the nanoparticle by incubation with proteases (Josephson, unpublished observations). Therefore immunoreactive FITC can be used as a surrogate to determine nanoparticle concentrations as we have done in Figures 2, 3, and 4, below.

The uptake of the Cp(FITC)–CLIO, Tat(FITC)–CLIO, and r8(FITC)–CLIO nanoparticles by CaCo-2 cells was examined by exposing monolayers to compounds, detaching the cells, and analyzing FITC-associated cell fluorescence by FACS. We employed two methods to express cell-associated, probe-based fluorescence: the percent of cells labeled is shown in Figure 1, and the relative median fluorescence (RMF) is shown below in Figure 2. RMF is the median fluorescence of labeled cells divided by the median fluorescence of unlabeled cells. The percent labeled cells after one- and four-hour incubation times with Cp(FITC)–CLIO (Figure 1 A), Tat(FITC)–CLIO (Figure 1 B), and r8(FITC)–CLIO (Figure 1 C) are shown, the vertical lines indicate the demarcation between labeled and unlabeled cells. The time course of cell labeling with the three nanoparticles (Figure 1 A–C) is summarized in Figure 1 D. A similar set of experiments was performed with the Cp(FITC), Tat(FITC), and r8(FITC) peptides (histograms not shown) and are summarized in Figure 1 E. It can be seen that nanoparticle uptake was strongly dependent on the nature of the attached peptide, with the amount of cell-associated fluorescence for r8(FITC)–CLIO greater than for Tat(FITC)–CLIO, which was greater than for Cp(FITC)–CLIO. Peptides r8(FITC) and Tat(FITC) rapidly became cell associated while Cp(FITC) was slow in this regard. It appears that the r8(FITC) and Tat(FITC) peptides labeled cells slightly faster than the corresponding nanoparticles, though our data do not permit an estimate of how much faster this labeling might be.

Data from the 4 hour time points of Figure 1 D and E are also shown in Figure 2 A, which compares the uptake as RMFs of our three peptide–nanoparticles and three corresponding peptides at 37 °C. The uptake for peptides was greatest for r8(FITC)–CLIO, then came Tat(FITC)–CLIO at $p < 0.05$, which was greater than Cp(FITC)–CLIO ($p < 0.01$). However, the major conclusion of Figure 2 A was that the RMFs of peptide–nanoparticles closely paralleled those of peptides. The RMFs of the Tat(FITC)/Tat(FITC)–CLIO pair and r8(FITC)/r8(FITC)–CLIO pair were not significantly different ($p > 0.05$). The RMFs for peptide–nanoparticles at 37 °C versus 4 °C are shown in Figure 2 B. The RMF of r8(FITC)–CLIO was higher at 37 °C than at 4 °C ($p < 0.01$), as was the RMF of Tat(FITC)–CLIO ($p < 0.01$). The low RMF of Cp(FITC)–CLIO was not dependent on temperature. The temperature dependence obtained suggests a metabolic-energy-dependent, endocytic mechanism for the transport of the Tat(FITC) and r8(FITC) nanoparticles, a result that is consistent with recent observations.[37,38] Finally, we compared the RMFs of CaCo-2 cells with earlier data on HeLa cells for Tat(FITC) and Tat(FITC)–CLIO, as shown in Figure 2 C.[36] The RMFs

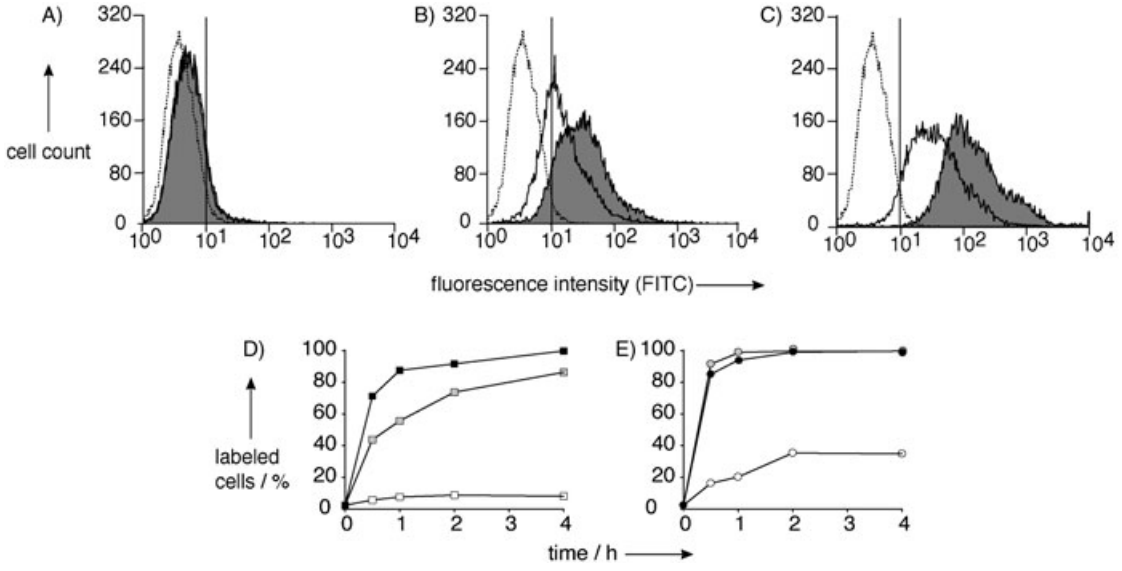

Figure 1. *Uptake of peptide–nanoparticle conjugates and peptides as determined by FACS. A), B), C) FACS histograms (frequency distribution) of CaCo-2 cells incubated with Cp(FITC)–CLIO (A), Tat(FITC)–CLIO (B), or r8(FITC)–CLIO (C) for 1 (white) or 4 h (black). The left distributions represent unlabeled control cells. The vertical line is the demarcation between labeled and unlabeled cells. D) and E) Percentage of labeled cells over time for peptide–nanoparticle conjugates (D) and, for comparison, unconjugated peptides (E). White: Cp(FITC)–CLIO and Cp(FITC), gray: Tat(FITC)–CLIO and Tat(FITC), black: r8(FITC)–CLIO and r8(FITC). Experiment shown is representative for two experiments.*

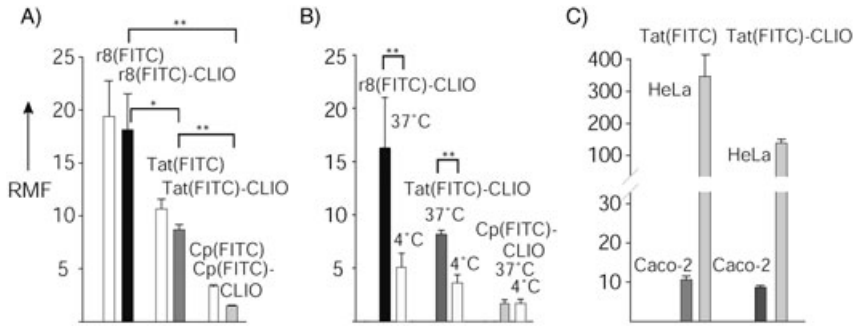

Figure 2. Uptake of peptide–nanoparticle conjugates and peptides by CaCo-2 cells. A) Peptide–nanoparticle and peptide uptake by Caco-2 cells (37°C, 4 h). B) Peptide–nanoparticle uptake at 4 or 37°C (4 h). C) Comparison of Tat(FITC) and Tat(FITC)–CLIO uptake in HeLa (37°C, 3 h) and CaCo-2 cells (37°C, 4 h). Cells were incubated with 10 (Caco-2) or 5 μM peptide (HeLa) either as peptide or as peptide–nanoparticle. Uptake is expressed as the RMF, calculated by dividing the median fluorescence intensity of the labeled cell population by the median fluorescence intensity of an untreated cell population. Student's t-test was performed A) to compare RMF values of r8(FITC)–CLIO, Tat(FITC)–CLIO and Cp(FITC)–CLIO and B) to compare values obtained at 4°C to 37°C for each peptide–nanoparticle conjugate ($p < 0.05$, **$p < 0.01$). Values are the mean ± SEM (n = 3).*

of HeLa cells exceeded those of CaCo-2 cells by over tenfold.

We next evaluated the permeation of peptide–nanoparticle conjugates and peptides across Caco-2 monolayers, as shown in Figure 3 using a recently developed immunoassay for fluorescein (see above). Monolayers had transepithelial electrical resistance (TEER) values of 651 ± 24 Ω cm^2 before and 641 ± 30 Ω cm^2 ($n = 25$) after the permeability experiments; this indicated no significant changes in the TEER values during these experiments. Cell-culture inserts without cells were not found to be a significant barrier for the permeation of peptide–nanoparticle conjugates (data not shown). We first determined the concentration-versus-time profiles when the concentration of materials in the donor compartment was constant for the duration of the experiment, as shown in Figure 3 A. The transport of peptides and peptide–nanoparticles was lower for the initial 9 h, and then increased in the period between 9 and 27 h. The percentages of nanoparticles traversing the monolayer at 27 h are given in Figure 3 B, and indicate that the permeation of nanoparticles was strongly dependent on the nature of the peptide attached, with Tat(FITC)–CLIO greater than Cp(FITC)–CLIO ($p < 0.05$). No statistically significant difference between r8(FITC)–CLIO and Tat(FITC)–CLIO (p value of 0.40) or between r8(FITC)–CLIO and Cp(FITC)–CLIO (p value of 0.38) was obtained, due to the high standard deviation for r8(FITC)–CLIO.

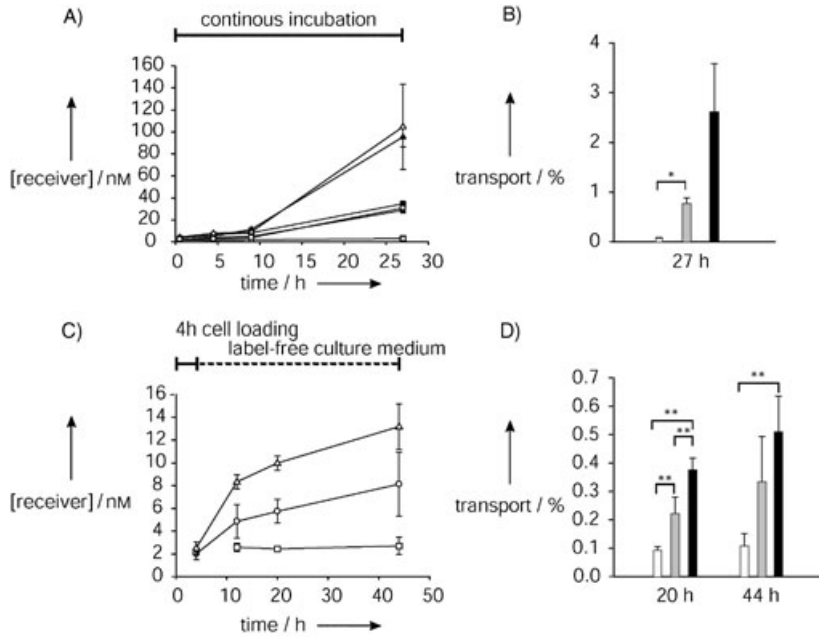

Figure 3. Permeation of peptide–nanoparticle conjugates across Caco-2 monolayers. Cells were incubated with Tat(FITC)–CLIO, r8(FITC)–CLIO, Cp(FITC)–CLIO, Tat(FITC), r8(FITC) or Cp(FITC). Concentration was 10 μM (referring to peptide). A) Time dependence of concentration in the receiver compartment. Contact between donor solution and monolayers was maintained for the full duration of the experiment (27 h). ○: Tat(FITC)–CLIO, ●: Tat(FITC), △: r8(FITC)–CLIO, ▲ r8(FITC), □: Cp(FITC)–CLIO, ■: Cp(FITC), squares. B) Percent of peptide–nanoparticles transported to receiver compartment after 27 h (from A). Black bar: r8(FITC)–CLIO, gray bar: Tat(FITC)–CLIO, white bar: Cp(FITC)–CLIO. C) Cells were incubated with peptides or peptide–nanoparticle conjugates for 4 h, then the donor solution was replaced with fresh cell-culture medium. Symbols as in (A). D) Percentage of peptide–nanoparticles transported to the receiver compartment after 20 and 44 h (from C). Bars coded as in (B). A) and B) Values are the mean ± SD (n = 4, experiment was performed in duplicate and analyzed twice). C) and D) Values are the mean ± SD (n = 3). Student's t-test was performed and related to Cp(FITC)–CLIO ($p < 0.05$, **$p < 0.01$).*

The P_{eff} values and molecular weights for the peptides and peptide–nanoparticles synthesized, together with those of the reference materials as derived from refs. [39, 40] are presented in Figure 4. The transport between the 9 and 27 hour incuba-

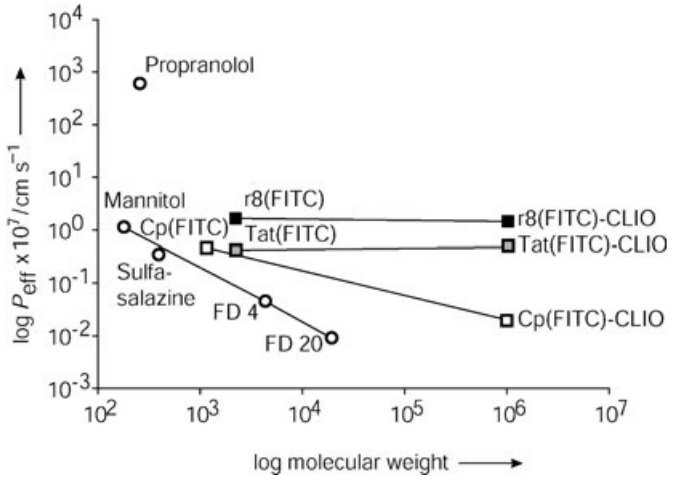

Figure 4. *Effective permeability versus molecular weight. P_{eff} of peptide–nanoparticle conjugates and unconjugated peptides in Caco-2 cells as calculated from the slope of the concentration time profile between 9 and 27 h. For comparison, literature values for propranolol, a well-absorbed drug, mannitol, a nonpermeable marker, and sulfasalazine are shown. Also shown is the dependency of effective permeability of mannitol and FITC–dextrans FD 4 and FD 20 on molecular weight (0.2, 4, and 20 kDa, respectively).*

tion times was used (data from Figure 3 A), and a constant concentration of donor material was assumed. The reference materials were mannitol, a poorly transported, low-molecular-weight substance, propranolol, a well-transported, low-molecular-weight substance, and FITC-labeled dextrans of 4 and 20 kDa, two poorly transported polymers. Also shown is sulfasalazine, a substrate for the P-glycoprotein (PGP) efflux pump.[41] The P_{eff} of the r8(FITC)–CLIO nanoparticle ($M_W \sim 1000$ kDa) was similar to that of mannitol, though the nanoparticle was about 5000 times larger on a weight basis. The P_{eff} of the r8(FITC)–CLIO and Tat(FITC)–CLIO nanoparticles were similar to those of the unconjugated peptides, though the nanoparticles were about 300 times bigger on a weight basis. The attachment of the r8(FITC) or Tat(FITC) peptides to the amino-CLIO nanoparticle yielded peptide–nanoparticles with P_{eff} values that were far higher than that obtained when Cp(FITC) was attached, again this indicated the ability of surface modification to control the transport of nanoparticles through CaCo-2 monolayers.

The intracellular localizations of Tat(FITC)–CLIO, r8(FITC)–CLIO, or Cp(FITC)–CLIO nanoparticles in CaCo-2 cells were examined by confocal microscopy, as shown in Figure 5. A strong surface fluorescence was found for Tat(FITC)–CLIO- and r8(FITC)–CLIO-treated cells, even after thorough washing with Hank's balanced salt solution (HBSS; Figure 5 A, D). No surface fluorescence was obtained with Cp(FITC)–CLIO (Figure 5 G). After the addition of trypan blue to quench surface fluorescence, internal cell fluorescence for cells incubated with r8(FITC)–CLIO (Figure 5 B) and Tat(FITC)–CLIO (Figure 5 E) was obtained, which was far weaker than the surface fluorescence. Fluorescence was cytoplasmic, displaying a punctuated pattern indicative of storage in vesicles, similar to that seen with Tat protein.[42] The unconjugated peptides showed a similar pattern, with high surface fluorescence, punctuated staining in the cytoplasm and occasionally nuclear uptake (data not shown).

Discussion

The current study is the first to demonstrate the ability of MTS peptides to affect the transfer of nanoparticles across monolayers and to compare the transport of MTS peptides with that of the MTS peptide–nanoparticle conjugates. Our data indicate that the transport of nanoparticles (defined as P_{eff}) through CaCo-2 monolayers can be dramatically altered through the attachment of MTS peptides. The attachment of r8(FITC) yielded a nanoparticle with a P_{eff} of 1.65×10^{-7} cm s^{-1}, which was about 80 times higher than the P_{eff} of the nanoparticle with a control peptide attached. The influence of peptide attachment largely overcame the negative effects of high nanoparticle molecular weight on monolayer transport. Thus the attachment of r8(FITC) to the CLIO nanoparticle yielded the r8(FITC)–CLIO nanoparticle ($M_W \sim 1000$ kDa), which had a P_{eff} similar to the r8(FITC) peptide and which was substantially higher than the

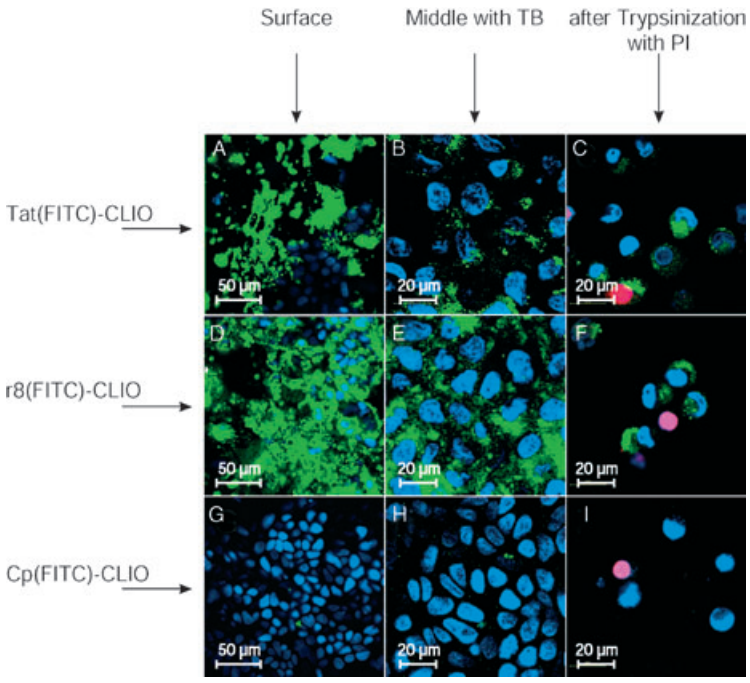

Figure 5. *Localization of peptide–nanoparticle conjugates in Caco-2 monolayers. Cells were treated with Tat(FITC)–CLIO (upper panels), r8(FITC)–CLIO (middle panels) or Cp(FITC)–CLIO (lower panels) for 4 h and washed with HBSS. Concentration was 10 µM (referring to peptide). Confocal sections were taken in living cells, from the surface of the monolayer (A, D, G), from the middle of the monolayer (B, E, H), or after trypsinization (C, F, I). In B, E, and H, trypan blue (TB) was added to reduce background fluorescence. In C, F, and I cells were trypsinized to reduce background fluorescence and propidium iodide (PI) was added to check for viability and cell membrane integrity.*

P_{eff} of much smaller (4 and 20 kDa) FITC-dextrans, as shown in Figure 5. The P_{eff} of the r8(FITC) peptide ($M_W \sim 2.221$ kDa) was in the range of P_{eff} values reported for mannitol ($M_W = 0.182$ kDa), with 1.2×10^{-7} cm s^{-1}[40] or 2.3×10^{-7} cm s^{-1}.[39,40] P_{eff} values were also compared with propranolol and sulfasalazine. However, the literature values used (Figure 5) were obtained after shorter incubations than we employed (up to 2 h).

We observed two phases of transport for both peptides and peptide–nanoparticles, a slow lag phase (0–8 h), followed by a faster, steady-state phase (9–27 h), as shown in Figure 3A, from which P_{eff} values were taken. A lag phase over time periods of up to 2–3 h has been seen with the transport of various substances through CaCo-2 monolayers.[43–47] A long lag phase of at least 3 h has been reported for the translocation of intact HIV virions through brain endothelial cell monolayers with a substantial increase in translocation after 24 and 48 h.[48] The mechanism of translocation was by lipid-raft-mediated macropinocytosis. Interestingly, the same mechanism has recently been identified for the cellular internalization of Tat conjugates.[49] Intact HIV virions have a diameter of about 100 nm,[50] comparable to our nanoparticle size of 49 nm.[36]

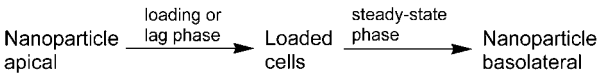

Scheme 2. *Uptake of nanoparticles by CaCo-2 monolayers.*

An initial lag phase in transport, followed by a faster steady-state phase, likely reflects the need to load cells with materials from the apical compartment over the initial hours (see Figure 3A), before the maximal rate of transport from iron-loaded cells to the basolateral medium occurs, as depicted in Scheme 2. The uptake of Tat(FITC) and Tat(FITC)–CLIO was higher for HeLa cells than CaCo-2 cells (Figure 2C), which may reflect a higher surface area for HeLa cells.

Using CaCo-2 cells, we observed a strong surface staining with Tat-like peptides and the corresponding nanoparticles (Figure 5), with minimal staining in the interior of the cells. In some studies with MDCK and CaCo-2 monolayers, however, a lack of intracellular fluorescence was obtained with fluorescent Tat peptides, see refs. [51, 52]. By contrast, with MDCK cells, a fluorescent Tat peptide showed punctuated cytoplasmic fluorescence.[53] Differences in the peptide sequences, cell culture, and other experimental details limit our ability to interpret theses discrepancies.

The transport of a Tc-labeled Tat peptide through CaCo-2 and MDCK monolayers has been studied by Violini et al.[52] Their P_{eff} values were for the initial two hours, whereas our P_{eff} values reflect transport after a lag phase and at 9–27 h after addition of the nanoparticle to the apical side of the monolayer (Figure 3A). Violini found that Tat peptide transport was similar to that of inulin, a poorly transported compound, and about 100-fold lower than that of propranolol, a well-transported compound. However, using CaCo-2 monolayers, Violini obtained higher P_{eff} values than usually reported for propranolol and higher P_{eff} values for the Tat peptide than we obtained. The reason for this discrepancy is not clear. They concluded that there was a permeation barrier to the transport of Tat peptide through well-differentiated cells. Trehin et al. also found little translocation of the Tat peptides through monolayers.[54] Lindgren et al., using a similar system to our, studied the permeability of penetratin, which, like the Tat-peptide, is a basic MTS peptide, and found 0.6% of the peptide passed through CaCo-2 cells in 2 h.[55] We obtained values for the Tat peptide and polyarginyl peptide of 0.7 and 2.4%, respectively, in 27 h, see Figure 3B.

It might be argued that the reliance on fluorescein, that is on fluorescein as determined by immunoassay, for our analytical method could lead to misleading conclusions. However, the design of the peptide–nanoparticle conjugates employed results in nanoparticles with very high chemical stability. The linkage between the FITC and the nanoparticle is not suitable for proteolytic attack because of the highly modified amino acid side chains used to link FITC to the nanoparticle, see Scheme 1. The cross-linking of dextran with epichlorohydrin to obtain the amino-CLIO nanoparticle to which peptides are attached results in a coating that remains bonded to the iron oxide even with temperatures as high as 121 °C.[56] After the internalization of the Tat(FITC)–CLIO nanoparticle by HeLa cells, the FITC linked to the nanoparticle was retained by cells in a manner similar to the retention of Cy3.5 attached directly to the dextran; this indicated that no separation of FITC from the nanoparticle occurred after internalization into HeLa cells.[36] Finally the rapid metabolism of peptide–nanoparticles to some minimal degradation product is inconsistent with the considerable differences in the transport of peptide–nanoparticles over long periods of time, see for example Figure 3A. Our results cannot eliminate the possibility of some peptide degradation with the peptide–nanoparticle conjugates. However, such degradation will not affect our central conclusion: the transport of the core nanoparticle (iron oxide, cross-linked dextran, fluorescein, see Scheme 1) through CaCo-2 monolayers can be greatly enhanced by the attachment of Tat-like membrane translocating peptides to that core.

The ability of surface modification to alter nanoparticle transport through a monolayer suggests several lines of future work. First, the synthesis of the surface-modified nanoparticles we employed can be done in a parallel fashion to rapidly synthesize positionally encoded libraries of surface-modified nanoparticles.[35] By determining the nanoparticle transport through monolayers with the nonisotopic FITC immunoassay, nanoparticles can be prepared in advance and stored before use in monolayer transport studies. These synthetic and analytic methods might permit a large body of data on nanoparticle transport to be generated (P_{eff} versus surface chemistry), perhaps leading to the design of nanoparticles with far higher P_{eff} values than those of the current study. A second conclusion regarding nanoparticle transport relates to the relatively long lag phase followed by a faster steady-state phase we obtained. This implies that substantial rates of nanoparticle transport may occur, if nanoparticles are exposed to the apical side of cells for long periods of time. While rapid transport through cells is needed for pharmaceuticals used to treat acute condi-

tions, more slowly absorbed pharmaceuticals could be equally useful. For example, the transcellular transport of topically applied agents, such as steroid hormones, can be a slow process and still provide therapeutic benefit. Enhanced internalization and transport might also be used in the design of immunogens, which, when used as vaccines, might require mucosal uptake. An understanding of the kinetics of nanoparticle internalization and transcellular transport, together with an understanding of the pharmacokinetics and therapeutic requirements of various therapeutic agents, can be used to select drugs that might benefit from the formulation into surface modified, nanoparticle based designs.

Experimental Section

Three peptide–nanoparticle conjugates were synthesized by using three peptides and named Tat(FITC)–CLIO, r8(FITC)–CLIO, and Cp(FITC)–CLIO. Peptides were synthesized by using Fmoc chemistry and modified by treatment with FITC as described.[18] Peptides were purified by reversed-phase HPLC and were within 1 Da of their expected mass by mass spectrometry. The peptides were: i) Tat(FITC), GRKKRRQRRRGYK(FITC)C-NH_2 (M_R 2237), ii) r8(FITC), GrrrrGrrrrGYK(FITC)C-NH_2 (M_R 2221), and iii) Cp(FITC), GDSDSGYK-(FITC)C-NH_2 (M_R 1156). Amino-CLIO was prepared as described.[18, 30]

Peptide–nanoparticle conjugates were prepared by adding amino-CLIO (4 mg, 0.071 mmol Fe) to *N*-succinimidyl iodoacetate, (SIA; 10 mg, 35 μmol, Molecular Bioscience, Boulder, CO, USA) in DMSO (200 μL). The mixture was vortexed, allowed to sit for 15 min, and purified with a PD-10 desalting column (Sigma–Aldrich, Buchs, Switzerland) in citrate (0.02 M) and NaCl (0.15 M), pH 8, to remove unreacted SIA. The activated amino-CLIO was then split into three equal amounts, and either Tat(FITC), r8(FITC), or Cp(FITC) (about 1 mg) in 0.1% *v/v* trifluoroacetic acid in water was added. The mixture was vortexed, allowed to react for 1–2 h, and purified with a PD-10 desalting column (Sigma–Aldrich). Unreacted peptide was removed by ultracentrifugation (Minicon YM-30, Millipore, Bedford, MA, USA) and dialysis (Spectrapor, MWCO 8000, Spectrum Europe B.V., Breda, The Netherlands). The number of attached FITC dyes per nanoparticle was determined spectrophotometrically (ϵ_{494} = 73 000). Iron was determined spectrophotometrically,[18] and the ratio of Tat(FITC), r8(FITC), and Cp(FITC) per nanoparticle was calculated by assuming 2064 iron atoms per CLIO particle.[57]

Cell monolayers: Caco-2 cells were purchased from ATCC (Manassas, VA, USA). Cells were cultured in DMEM (Dulbecco's modified Eagles Medium) with glucose (4.5 mg mL^{-1}), containing 20% fetal bovine serum (FBS) for the first two passages after thawing, and 10% FBS for further maintenance. Medium was supplemented with penicillin (100 U mL^{-1}), streptomycin (100 μg mL^{-1}), Na-pyruvate (1 mM), L-glutamine (2 mM), and nonessential amino acids (0.1 mM). Media, balanced salt solutions and supplements were from Cellgro (Mediatech Inc, Herndon, VA, USA). Cells were cultured and passaged according to standard conditions.[58] Confluent and differentiated Caco-2 cells were used for experiments at days 18–21. Passage numbers used were 20–30. The medium was exchanged three times a week.

For cell transport/permeability studies, cells were seeded on cell-culture inserts (polyethylene terephthalate; PET), 1 μm pore size, 1.6×10^6 pores per cm^2, 0.9 cm^2 growth area) and companion plates (12-well plates, Falcon, Becton Dickinson, Franklin Lakes, NJ, USA) with a density of 10^5 cells per cm^2. Cells were kept with medium (1.5 mL) in the basolateral chamber and with medium (0.5 mL) in the apical chamber. The integrity of the Caco-2 cell monolayer was evaluated by measuring the TEER. TEER is represented as resistance in Ω cm^2, corrected for the blank filter and normalized for surface area with an epithelial tissue voltohmmeter (Evom, Hilton, South Australia). Cells had a resistance between 600 and 700 Ωcm^2. Microscopy studies were performed on glass chamber slides (Lab-Tek Chambered Coverglass, Nalge Nunc, Naperville, IL, USA) and flow cytometry (FACS) in cell-culture inserts or on 24-well plates (Falcon). Cell density was identical to that used for permeability studies.

For FACS, cells were incubated with Tat(FITC)–CLIO, r8(FITC)–CLIO, or Cp(FITC)–CLIO nanoparticles at 10 μM peptide concentration, which corresponds to 50 μg Fe mL^{-1}, or with unconjugated Tat-(FITC), r8(FITC), or Cp(FITC) peptides (10 μM). Conjugates and peptides were added to complete cell-culture medium. The medium was sterile-filtered (0.2 μm pore size, low protein binding, Gelman, Ann Arbor, MI, USA) before addition to cells. After incubation, cells were washed with HBSS (4×) and trypsinized for 15 min. Trypsinization was stopped by addition of cold DMEM containing 20% FCS. Cells were separated by pipetting up and down for several times and transferred to FACS tubes (Becton Dickinson), spun down, washed with HBSS (2×), and fixed in 2% paraformaldehyde (Sigma–Aldrich) in HBSS. Cells were analyzed by FACS on a FacsCalibur (Becton Dickinson, Franklin Lakes, NJ, USA). A total of 10 000 cells per sample were analyzed. The number of cells with a fluorescence intensity higher than that of unlabeled cells was used to calculate the percent of labeled cells. The baseline was determined by analyzing unlabeled control cells. RMF (relative median fluorescence) was calculated by dividing the median of the labeled cells by the median of an unlabeled cell population.

For confocal-laser scanning microscopy (CLSM), cells were incubated with Tat(FITC)–CLIO, r8(FITC)–CLIO, Cp(FITC)–CLIO, or unconjugated Tat(FITC), r8(FITC), or Cp(FITC) peptides (10 μM) for 4 h at 37 °C in complete cell-culture medium. After 3.5 h, the medium was removed and replaced by Hoechst 33342 (10 μM; Molecular Probes) in HBSS. After 30 min, the cells were washed with HBSS (4×) and examined by CLSM (Zeiss 410 inverted microscope, Zürich, Switzerland). Two-dimensional multichannel image processing was performed by using the IMARIS software (Bitplane AG, Switzerland). The background fluorescence of the cells was determined by analyzing unlabeled cells.

To more clearly view intracellular fluorescence, trypan blue was used to quench surface FITC fluorescence.[59–61] Half of the volume (0.2 mL) was replaced with 0.4% trypan blue before CLSM.

To check for membrane integrity of the cells after 4 h incubation with peptide nanoparticle conjugates, cells were trypsinized and detached as described for FACS. Suspensions were then incubated with propidium iodide (30 μg mL^{-1}; Molecular Probes, Leiden, the Netherlands) in HBSS for 5 min, spun down again, and resuspended in cell-culture medium. Cells were allowed to settle down on a glass chamber slide for 3 h and examined by CLSM without prior fixation.

Monolayer permeability was measured in complete cell-culture medium across cell layers grown on PET cell-culture inserts in 12-well plates. Conjugates or peptides (0.4 mL) as donor solutions were added to the apical side, and of cell-culture medium (1.5 mL) to the basolateral side. The study was performed under normal culture conditions (37 °C, 5% CO_2 containing O_2). The integrity of the cell culture layers was monitored before and after each permeability study by measuring the TEER.

Two experimental designs were used to measure cell permeability. For the first, peptides or peptide–CLIO conjugates were placed on the cells, and transport was monitored continuously for 27 h (Figure 3A). In the second, peptides or peptide–nanoparticle conjugates were placed on the apical side for 4 h, and replaced with cell-culture medium. After 4 h, cells were washed with medium (3×) and incubated for a further 44 h. Samples were taken out of the receiver solution after 4, 12, 20, and 44 h (Figure 3C). Both designs used 0.4 mL of Tat(FITC)–CLIO, r8(FITC)–CLIO, Cp(FITC)–CLIO nanoparticles or Tat(FITC), r8(FITC), or Cp(FITC) peptides at 10 μM peptide added to the apical side of the insert. The amounts of nanoparticles transported were obtained by applying corrections for sample removed.

In order to be able to compare our results to other studies that made use of CaCo-2 monolayers, a linear rise in concentration between 9 and 27 h was assumed, and an estimation of an effective permeability coefficient P_{eff} between 9 and 27 h was calculated according to Equation 1:

$$P_{eff} = \left(\frac{dC}{dt}\right)_{ss} \frac{V}{A \cdot C_D} \quad (1)$$

Here $(dC/dt)_{ss}$ is the steady-state slope of the concentration versus time profile in the receiver compartment, A is the cross-sectional area of the filter membrane, V is the volume of the receiver chamber, and C_D is the initial concentration in the donor compartment. The donor concentrations used to calculate P_{eff} were 10 μM, as initially added to the apical side. Donor concentrations for r8(FITC), Tat(FITC), r(8)FITC-CLIO, and Tat(FITC)–CLIO decreased in the apical medium by about 50% during the 27 h experiment—presumably due to surface attachment to and internalization into cells—whereas donor concentrations in the apical solution were maintained for Cp(FITC) and Cp(FITC)–CLIO. For simplicity, constant donor concentrations were used for the calculation of P_{eff}, even though effective permeability values might be underestimated.

Additionally, the percentage of permeated substance was determined. The absolute amount in the donor chamber was set at 100%, and the ratio of absolute permeated amount to the receiver was calculated. P_{eff} has units of $cm\,s^{-1}$.

For peptides and peptide–nanoparticle conjugates, determination of the concentrations of transported materials was based on fluorescein, whose concentrations were determined by using an enzyme immunoassay that permits the concentrations of both peptides and peptide–nanoparticles to be determined by one single nonisotopic method that is more sensitive than direct fluorescence. The assay uses FITC-BSA-coated (BSA = bovine serum albumin) microtiter plates and an anti-FITC horseradish peroxidase (HRP). It is run in competitive format, see Figure 1 of ref. [31], in which FITC in the sample reduces the attachment of the anti-FITC HRP conjugate to the solid-phase FITC. Briefly, at the respective time points, cell-culture medium (50 μL) was removed from the basolateral side of the insert and diluted 1:10 four times in 0.1% BSA. The diluted solutions were first treated overnight at 4°C with an anti-FITC horseradish peroxidase conjugate (40 $ng\,mL^{-1}$; Molecular Probes), and the mixture was then transferred onto a 96-well plate (MaxiSorp, Nunc; 200 μL per well) coated with FITC-labeled BSA (12.5 $ng\,mL^{-1}$; Sigma Chemical). Plates were then washed three times (PBS, 0.1% BSA, 0.1% Triton X-100), and horseradish peroxidase activity was quantitated at 650 nm by using 3,3′,5,5′-tetramethylbenzidine dihydrochloride (200μL; TMB, Sigma) after 30 min incubation at room temperature. Iron concentrations of the appropriate dilution (1:100 or 1:1000) of the samples were calculated from a standard curve by using nanoparticle standards in 0.1% aqueous BSA solution. A more complete description of the FITC immunoassay method has recently been published.

Keywords: drugs · iron · nanomaterials · particles · peptides

[1] J. Kreuter, *Adv. Drug Delivery Rev.* **2001**, *47*, 65.
[2] U. Schroeder, P. Sommerfeld, S. Ulrich, B. A. Sabel, *J. Pharm. Sci.* **1998**, *87*, 1305.
[3] L. A. Dailey, E. Kleemann, M. Wittmar, T. Gessler, T. Schmehl, C. Roberts, W. Seeger, T. Kissel, *Pharm. Res.* **2003**, *20*, 2011.
[4] A. M. Dyer, M. Hinchcliffe, P. Watts, J. Castile, I. Jabbal-Gill, R. Nankervis, A. Smith, L. Illum, *Pharm. Res.* **2002**, *19*, 998.
[5] J. C. Leroux, R. Cozens, J. L. Roesel, B. Galli, F. Kubel, E. Doelker, R. Gurny, *J. Pharm. Sci.* **1995**, *84*, 1387.
[6] M. P. Desai, V. Labhasetwar, G. L. Amidon, R. J. Levy, *Pharm. Res.* **1996**, *13*, 1838.
[7] F. Delie, *Adv. Drug Delivery Rev.* **1998**, *34*, 221.
[8] C. Santos Maia, W. Mehnert, M. Schaller, H. C. Korting, A. Gysler, A. Haberland, M. Schafer-Korting, *J. Drug Targeting* **2002**, *10*, 489.
[9] M. Simeonova, R. Velichkova, G. Ivanova, V. Enchev, I. Abrahams, *Int. J. Pharm.* **2003**, *263*, 133.
[10] Z. Mei, H. Chen, T. Weng, Y. Yang, X. Yang, *Eur. J. Pharm. Biopharm.* **2003**, *56*, 189.
[11] J. B. Rothbard, S. Garlington, Q. Lin, T. Kirschberg, E. Kreider, P. L. McGrane, P. A. Wender, P. A. Khavari, *Nat. Med.* **2000**, *6*, 1253.
[12] K. E. Bullok, M. Dyszlewski, J. L. Prior, C. M. Pica, V. Sharma, D. Piwnica-Worms, *Bioconjugate Chem.* **2002**, *13*, 1226.
[13] M. Nakanishi, A. Eguchi, T. Akuta, E. Nagoshi, S. Fujita, J. Okabe, T. Senda, M. Hasegawa, *Curr. Protein Pept. Sci.* **2003**, *4*, 141.
[14] E. L. Snyder, S. F. Dowdy, *Curr. Opin. Mol. Ther.* **2001**, *3*, 147.
[15] H. Xia, Q. Mao, B. L. Davidson, *Nat. Biotechnol.* **2001**, *19*, 640.
[16] M. Lewin, N. Carlesso, C. H. Tung, X. W. Tang, D. Cory, D. T. Scadden, R. Weissleder, *Nat. Biotechnol.* **2000**, *18*, 410.
[17] M. F. Kircher, J. R. Allport, E. E. Graves, V. Love, L. Josephson, A. H. Lichtman, R. Weissleder, *Cancer Res.* **2003**, *63*, 6838.
[18] L. Josephson, C. H. Tung, A. Moore, R. Weissleder, *Bioconjugate Chem.* **1999**, *10*, 186.
[19] M. Zhao, M. F. Kircher, L. Josephson, R. Weissleder, *Bioconjugate Chem.* **2002**, *13*, 840.
[20] R. Bhorade, R. Weissleder, T. Nakakoshi, A. Moore, C. H. Tung, *Bioconjugate Chem.* **2000**, *11*, 301.
[21] S. Futaki, T. Suzuki, W. Ohashi, T. Yagami, S. Tanaka, K. Ueda, Y. Sugiura, *J. Biol. Chem.* **2001**, *276*, 5836.
[22] S. Fawell, J. Seery, Y. Daikh, C. Moore, L. L. Chen, B. Pepinsky, J. Barsoum, *Proc. Natl. Acad. Sci. USA* **1994**, *91*, 664.
[23] H. J. Lee, W. M. Pardridge, *Bioconjugate Chem.* **2001**, *12*, 995.
[24] S. R. Schwarze, A. Ho, A. Vocero-Akbani, S. F. Dowdy, *Science* **1999**, *285*, 1569.
[25] V. P. Torchilin, *Cell Mol. Biol. Lett.* **2002**, *7*, 265.
[26] D. J. Mitchell, D. T. Kim, L. Steinman, C. G. Fathman, J. B. Rothbard, *J. Pept. Res.* **2000**, *56*, 318.
[27] S. Futaki, *Int. J. Pharm.* **2002**, *245*, 1.
[28] E. Vives, C. Granier, P. Prevot, B. Lebleu, *Lett. Pept. Sci.* **1997**, *4*, 1.
[29] J. M. Perez, L. Josephson, T. O'Loughlin, D. Hogemann, R. Weissleder, *Nat. Biotechnol.* **2002**, *20*, 816.
[30] L. Josephson, J. M. Perez, R. Weissleder, *Angew. Chem.* **2001**, *113*, 3304; *Angew. Chem. Int. Ed.* **2001**, *40*, 3204.
[31] K. A. Kelly, F. Reynolds, R. Weissleder, L. Josephson, *Anal. Biochem.* **2004**, *330*, 181.
[32] P. Wunderbaldinger, L. Josephson, R. Weissleder, *Bioconjugate Chem.* **2002**, *13*, 264.
[33] P. Artursson, K. Palm, K. Luthman, *Adv. Drug Delivery Rev.* **2001**, *46*, 27.
[34] G. Wilson, *Eur. J. Drug Metab. Pharmacokinet.* **1990**, *15*, 159.
[35] E. A. Schellenberger, F. Reynolds, R. Weissleder, L. Josephson, *ChemBioChem* **2004**, *5*, 275.
[36] A. M. Koch, F. Reynolds, M. F. Kircher, H. P. Merkle, R. Weissleder, L. Josephson, *Bioconjugate Chem.* **2003**, *14*, 1115.

[37] E. Vives, J. P. Richard, C. Rispal, B. Lebleu, *Curr. Protein Pept. Sci.* **2003**, *4*, 125.
[38] J. S. Wadia, R. V. Stan, S. F. Dowdy, *Nature Med.* **2004**, *10*, 310.
[39] J. Karlsson, P. Artursson, *Int. J. Pharm.* **1991**, *71*, 55.
[40] T. Lindmark, N. Schipper, L. Lazorova, A. G. de Boer, P. Artursson, *J. Drug Targeting* **1998**, *5*, 215.
[41] E. Liang, J. Proudfoot, M. Yazdanian, *Pharm. Res.* **2000**, *17*, 1168.
[42] D. A. Mann, A. D. Frankel, *EMBO J.* **1991**, *10*, 1733.
[43] I. J. Hidalgo, R. T. Borchardt, *Biochim. Biophys. Acta* **1990**, *1028*, 25.
[44] M. E. Taub, W. C. Shen, *J. Cell Sci.* **1993**, *106*(4), 1313.
[45] P. J. Chikhale, R. T. Borchardt, *Drug Metab. Dispos.* **1994**, *22*, 592.
[46] A. R. Kamuhabwa, P. Augustijns, P. A. de Witte, *Int. J. Pharm.* **1999**, *188*, 81.
[47] V. Tantishaiyakul, K. Wiwattanawongsa, S. Pinsuwan, S. Kasiwong, N. Phadoongsombut, S. Kaewnopparat, N. Kaewnopparat, Y. Rojanasakul, *Pharm. Res.* **2002**, *19*, 1013.
[48] N. Q. Liu, A. S. Lossinsky, W. Popik, X. Li, C. Gujuluva, B. Kriederman, J. Roberts, T. Pushkarsky, M. Bukrinsky, M. Witte, M. Weinand, M. Fiala, *J. Virol.* **2002**, *76*, 6689.
[49] J. S. Wadia, S. F. Dowdy, *Curr. Protein Pept. Sci.* **2003**, *4*, 97.
[50] G. Raposo, M. Moore, D. Innes, R. Leijendekker, A. Leigh-Brown, P. Benaroch, H. Geuze, *Traffic* **2002**, *3*, 718.
[51] S. D. Kramer, H. Wunderli-Allenspach, *Biochim. Biophys. Acta* **2003**, *1609*, 161.
[52] S. Violini, V. Sharma, J. L. Prior, M. Dyszlewski, D. Piwnica-Worms, *Biochemistry* **2002**, *41*, 12652.
[53] R. Trehin, U. Krauss, R. Muff, M. Meinecke, A. G. Beck-Sickinger, H. P. Merkle, *Pharm. Res.* **2004**, *21*, 33.
[54] R. Trehin, U. Krauss, A. G. Beck-Sickinger, H. P. Merkle, M. N. Nielsen, *Pharm. Res.* **2004**, *7*, 1248.
[55] M. E. Lindgren, M. M. Hallbrink, A. M. Elmquist, U. Langel, *Biochem. J.* **2004**, *377*, 69.
[56] S. Palmacci, L. Josephson, US Patent 5262176, **1993**.
[57] T. Shen, R. Weissleder, M. Papisov, A. Bogdanov, Jr., T. J. Brady, *Magn. Reson. Med.* **1993**, *29*, 599.
[58] P. Artursson, J. Karlsson, G. Ocklind, N. Schipper in *Epithelial Cell Culture* (Ed.: A. J. Shaw), Oxford University Press, New York, **1996**, p. 111.
[59] S. Sahlin, J. Hed, I. Rundquist, *J. Immunol. Methods* **1983**, *60*, 115.
[60] C. P. Wan, C. S. Park, B. H. Lau, *J. Immunol. Methods* **1993**, *162*, 1.
[61] Z. Ma, L. Y. Lim, *Pharm. Res.* **2003**, *20*, 1812.

Received: May 27, 2004
Published online: January 13, 2005

